YU ISSN 0015—3206
FZKAAA 22 (1) 233 (1990)

PROTON-NEUTRON MULTIPLETS IN ODD-ODD Tl NUCLEI

JORIS VAN MALDEGHEM+ and KRIS HEYDE

Institute for Nuclear Physics and Institute for Theoretical Physics, Proeftuinstraat 86, B 9000 Gent, Belgium

Received 29 September 1989

UDC 539.142

Original scientific paper

Making use of the ideas of particle-core coupling as applied to the study of odd-odd nuclei, a detalied description of nuclear structure in the $^{186-200}_{81}$Tl nuclei is given. The importance of the proton-neutron interaction is emphasized in outlining multiplets for specific proton and neutron orbitals. It is also shown how particle-core quadrupole coupling induces an »effective« proton-neutron quadrupole force with a quadratic dependence on the multiplet angular momentum i. e. the parabolic rule is regained.

1. Introduction

In the last few years, the amount of information on odd-odd nuclei in the $Z = 50$ and $Z = 82$ region has been extended considerably. With the help of heavy-ion reactions, the existence of collective bands was established. The study of such bands confirms our knowledge of collective behaviour as deduced from the study of the neighbouring even-even and odd-mass nuclei. In addition, it enables us to draw conclusions about the residual proton-neutron interaction.

In order to study collective bands in odd-odd nuclei, we make use of an approach based on proton-neutron multiplets coupled to the quadrupole vibrations of the underlying core. The concept of particle-core coupling, which is very elegant and simple in principle has been developed mainly at Zagreb under the guidance of Prof. Alaga. The realm of applications of this concept in both odd-mass, even-even and odd-odd nuclei is very extended and bears about on every mass region

+ Permanent address: MCC nv, Fr. Laurentplein 25, 9000 Gent (Belgium).

from light to heavy nuclei (see Ref. 1 and refs. therein). A short outline of this approach is given in Section 2. There, we also concentrate on the behaviour of a specific proton-neutron multiplet in the presence of collective vibrations. In Sect. 3, a detailed application to odd-odd nuclei in the $Z = 82$ region i. e. the Tl isotopes is performed.

2. *Model description*

The general form of the Hamiltonian describing odd-odd nuclei can be written as

$$H = H_{coll} + H_{qp}(\pi) + H_{qp}(\nu) + H_{coupl}(\pi) + \\ + H_{coupl}(\nu) + H_{int}(\pi, \nu), \tag{2.1}$$

where

$$H_{coll} = \hbar\omega_2 \sum_{\mu} (b^+_{2\mu}\, b_{2\mu} + 1/2), \tag{2.2}$$

describes the excitation energy of the underlying vibrational core ($b^+_{2\mu}$ denotes the quadrupole phonon creation operator, $\hbar\omega_2$ the quadrupole phonon energy), and

$$H_{qp}(\varrho) = \sum_{nljm} E_{nlj}(\varrho)\, N(c^+_{nljm}(\varrho)\, c_{nljm}(\varrho)), \qquad (\varrho = \pi, \nu) \tag{2.3}$$

describes the unperturbed quasiparticle energy of the proton (neutron). Here, $E_{nlj}(\varrho)$ denotes the proton (neutron) quasiparticle energy, $c^+_{nlj}(\varrho)$ the proton (neutron) quasiparticle operator, and $N(\ldots)$ indicates the normal ordering with respect to the proton (neutron) Bardeen-Cooper-Schrieffer (BCS) vacuum. $H_{coupl}(\varrho)$ describes the coupling between the proton (neutron) fermion degrees of freedom and the quadrupole vibrations. The explicit expression is yiven by

$$H_{coupl}(\varrho) = -\sqrt{\frac{\pi}{5}}\, \xi_2(\varrho)\, \hbar\omega_2 \sum_{\substack{n'l'j'm'\mu \\ nljm}} (b_{2\mu} + (-1)^{\mu} b^+_{2-\mu}) \times \\ \times \langle nljm(\varrho) \,|\, Y_{2\mu} \,|\, n'l'j'm'(\varrho)\rangle \cdot N(c^+_{nljm}(\varrho)\, c_{n'l'j'm'}(\varrho)). \tag{2.4}$$

Finally $H_{int}(\pi, \nu)$ describes the remaining residual interaction between protons and neutrons.

To obtain energy spectra and wave functions, the Hamiltonian is diagonalized in the basis spanned by proton-neutron multiplets coupled to the collective quadrupole excitations of the underlying core. Consequently the final wave functions can be expanded as:

$$|J_i M\rangle = \sum_{NRI_k} d^i(NRI; J)\, |(N, R) \times [nlj(\pi) \times n'l'j'(\nu)]\, I_k; JM\rangle, \tag{2.5}$$

where N represents the number of quadrupole phonons, R is the angular momentum of the quadrupole phonons, and $[nlj(\pi) \times n'l'j'(\nu)]\, I_k$ denotes the proton-neutron multiplet coupled to the total angular momentum I. If $N \geq 4$, an additio-

nal quantum number is required to label uniquely the N-quadrupole phonon state.

In order to obtain the quasiparticle energies and the occupation probabilities v^2, a BCS calculation was performed using the Nilsson Hamiltonian plus pairing force[2]. The values of μ and $\varkappa$ were taken from Ref. 3.

Starting from a microscopic $Q_2(\pi) \cdot Q_2(\nu)$ interaction between the valence particles, one can understand the macroscopic vibrational core-particle Q_2 (coll) · · Q_2 (particle) interaction[4]. The latter interaction also causes an energy splitting of a p-n multiplet, in addition to the »direct« p-n interaction. Ignoring the p-n interaction, the energy splitting of a quasi-proton quasi-neutron multiplet due to the quadrupole coupling Q_2 (coll) · Q_2 (particle) to the core, is given, in second order perturbation theory, by the parabolic rule[5].

Taking the coupling term explicitely as:

$$H_{coupl} = -\sqrt{\frac{\pi}{5}}\,\hbar\omega_2\,(\xi_2(\pi)\,Y_2(\pi) + \xi_2(\nu)\,Y_2(\nu)) \cdot Q_2(coll), \tag{2.6}$$

with

$$Q_{2\mu}(coll) = b^+_{2\mu} + (-1)^\mu\, b_{2-\mu}, \tag{2.7}$$

$b^+_{2\mu}$ = quadrupole phonon creation operator,

one can derive the corresponding second order energy splitting (parabolic rule):

$$\Delta E(I) = \frac{-2\pi}{5}\,\Theta(p)\,\Theta(n)\,\xi(\pi)\,\xi(\nu)\,\hbar\omega_2\,(-1)^{j_p+j_n+I} \begin{Bmatrix} j_p & j_n & I \\ j_n & j_p & 2 \end{Bmatrix} \times$$
$$\times \langle j_p||Y_2||j_p\rangle \langle j_n||Y_2||j_n\rangle, \tag{2.8}$$

with

$$\Theta(w) = (u_w^2 - v_w^2) \qquad w = p, n.$$

We refer to Appendix A for more details. There, we also show that $\Delta E(I)$ represents a parabola as a function of $I(I+1)$. Moreover, the energy splitting depends on the product $\xi_2(\pi) \cdot \xi_2(\nu)$ of the coupling strengths.

In carrying out a detailed study of the above methods for the odd-odd Tl nuclei, the parabolic rule and the dramatic effects caused by particle-core coupling will be highlighted.

3. *Applications to* $^{186-200}Tl$

3.1. *Introduction*

In the odd-odd $^{186-200}$Tl isotopes, a negative parity band starting with $J^\pi = 8^-\,(9^-, 10^-)$ and based on the $1h_{9/2}(\pi) - 1\tilde{i}_{13/2}(\nu)$ intruder multiplet has been identified[6-13]. Detailed calculations were performed within the frame work of the two-quasiparticle plus rotor model (TQPRM) eventually including a proton-neutron interaction[6-13]. The present situation can be summarized as follows:

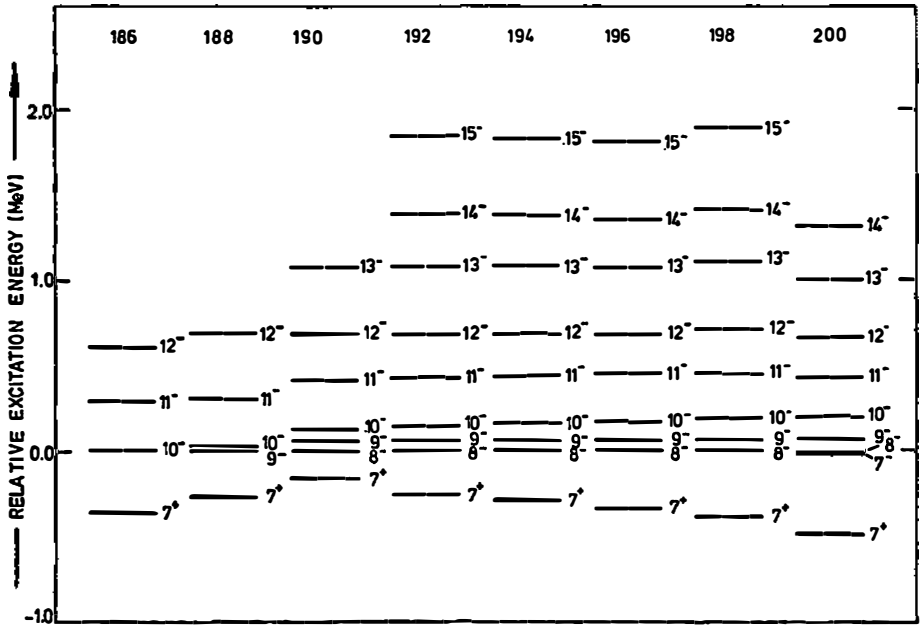

Fig. 1a. Experimentally determined negative parity band in the $^{186-200}$Tl isotopes. Energy levels known up to 2 MeV above the bandhead are shown. The bandhead decays into the 7^+ isomer. The latter is also drawn.

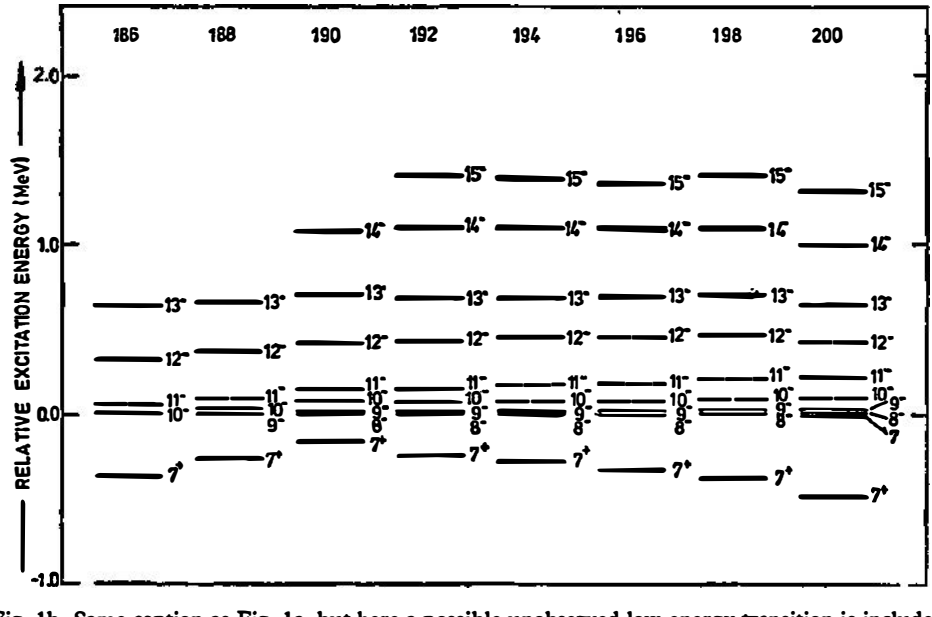

Fig. 1b. Same caption as Fig. 1a, but here a possible unobserved low-energy transition is included in the level scheme (see detailed values in Table 2).

(i) The band starts with a set of transitions whose energies are unusually small as compared to energies in related bands (i. e. $1h_{9/2}$ (π) intruder and $\tilde{1}i_{13/2}$ (ν) bands in odd Tl and Hg nuclei, respectively). It is therefore experimentally not easy to resolve the lower members of the multiplet. Owing to this experimental uncertainty, unobserved low-energy transitions could have escaped observation. This opens two possibilities for constructing the corresponding level schemes (Figs. 1.a and 1.b):

— we assume that *all* gamma transitions within the band have been observed, giving the spectrum of Fig. 1.a (the gamma transition are given explicitely in Table 1)

TABLE 1.

A	186	188	190	192	194	196	198	200
8^-								0.003
9^-			0.063	0.060(+)	0.060(+)	0.062	0.071	0.076
10^-		0.034	0.070(+)	0.083	0.096	0.109	0.122	0.119
11^-	0.276	0.273	0.273	0.276	0.278	0.271	0.259	0.217
12^-	0.322	0.302	0.281	0.262	0.245	0.236	0.246	0.230
13^-			0.382	0.396	0.403	0.397	0.402	0.348
14^-				0.309	0.283	0.267	0.297	0.311

Transition energies $\Delta E(I) = E(I) - E(I-1)$ (in MeV) in the negative parity band in $^{186-200}$Tl isotopes. No unobserved low energy transition is included.
(+) = estimated values (by extrapollation of systematics)

— since experimentally very low gamma transitions might have escaped detection, upper limits are given in almost all odd-odd Tl nuclei. In constructing the spectrum of Fig. 1.b, we *assume* energies for these transitions conform with the upper limit to exist and as given in Table 2.

TABLE 2.

	186	188	190	192	194	196	198	200
8^-								0.003
9^-			0.015(*)	0.014(*)	0.013(*)	0.012(*)	0.011(*)	0.010(*)
10^-		0.034	0.063	0.060(+)	0.060(+)	0.062	0.071	0.076
11^-	0.050(+)	0.060(+)	0.070(+)	0.083	0.096	0.109	0.122	0.119
12^-	0.276	0.273	0.273	0.276	0.278	0.271	0.259	0.217
13^-	0.322	0.302	0.281	0.262	0.245	0.236	0.246	0.230
14^-			0.382	0.396	0.403	0.397	0.402	0.348
15^-				0.309	0.283	0.267	0.297	0.311

Transition energies $\Delta E(I) = E(I) - E(I-1)$ (in MeV) in the negative parity band in $^{186-200}$Tl isotopes. An unobserved low energy transition is included.
(+) = estimated values (by extrapolation of systematics)
(*) = value equal to the experimentally determined upper limit

(ii) The negative parity band displays a smooth neutron-number dependence. We observe a compression of the first excited states of the band (8^-, 9^-, 10^-, (11^-)), with decreasing neutron-number, leading to level crossings of the bandhead for the lighter Tl isotopes.

(iii) In Tables 1 and 2, the transition energies $\Delta E_I \equiv E_I - E_{I-1}$ of the negative parity band are given. Restricting ΔE_I (with $I = 10 + \Delta I$, $11 + \Delta I$, $12 + \Delta I$, $13 + \Delta I$ and $14 + \Delta I$, $\Delta I = 0$ or 1) to $A = 192$, 194, 196, 198, staggering is detected (Fig. 2). Here $\Delta I = 1$ corresponds to the case where an

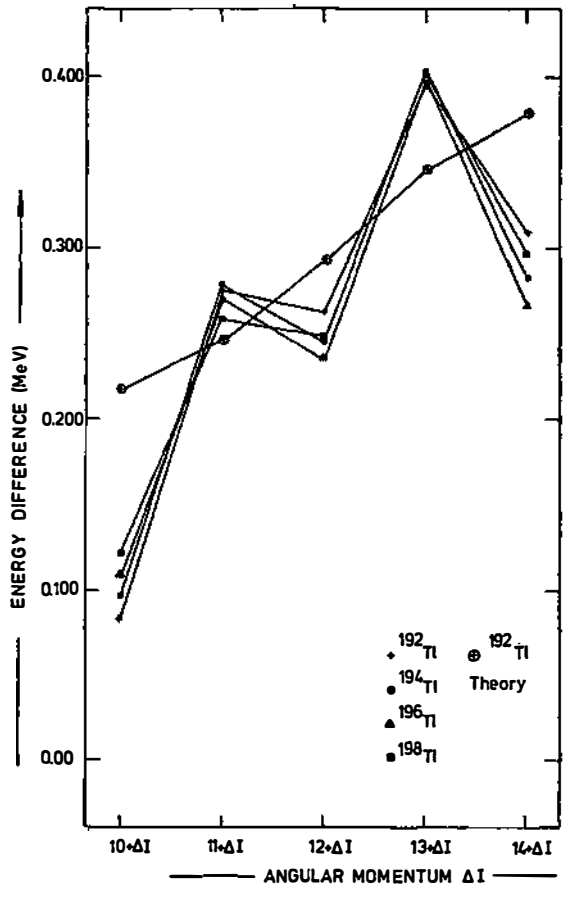

Fig. 2. Experimental energy difference $E_I - E_{I-1}$ for $^{192-198}$Tl for $I = 10 + \Delta I$, $11 + \Delta I$, ..., $14 + \Delta I$. The experimental trend shows staggering. This is not confirmed by the theoretical calculation for ^{192}Tl, as shown in the figure.

unobserved low-energy transition is included (see energies in Table 2), whereas taking $\Delta I = 0$ means no unobserved transition is accounted for (see energies in Table 1). The two cases ($\Delta I = 0$ or 1) correspond to an opposite phase of staggering. Should no additional transition be present, the simple

two-noninteracting quasiparticle plus rotor model would be insufficient to explain the observed staggering[12]. The inclusion of a proton-neutron interaction explains the staggering through a $(-1)^I$ dependence of the proton-neutron force (Figs. 1.a, b). Here $\vec{I}$ being the total intrinsic angular momentum $\vec{I} = \vec{j}_\pi + \vec{j}_\nu$. On the other hand, a systematic comparsion of the doubly-odd Tl isotopes and the neighbouring odd-Tl and even-even Hg isotopes (Fig. 3) provides strong evidence supporting the interpretation that the

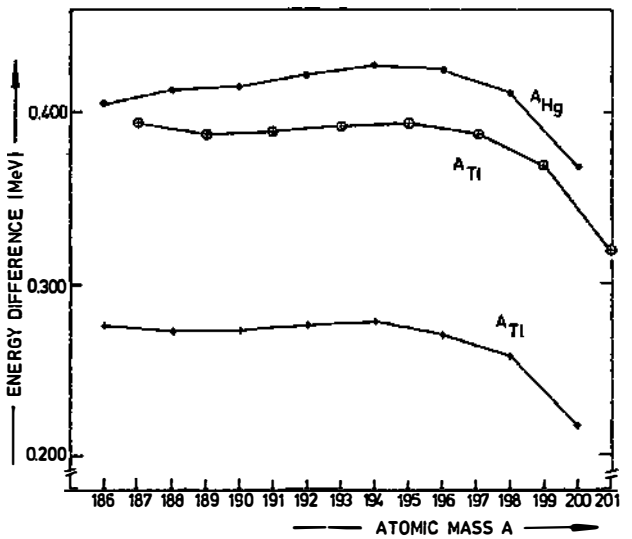

Fig. 3. The energy differences $'E(2^+) - E(0^+_1)$; $E(11^- + \Delta I) - E(10^- + \Delta I)$ and $E(11/2^-) - E(9/2^-)$ in respectively the even-even Hg, odd-odd Tl and the odd-even Tl isotopes. The experimental trends are shown as a function of mass-number.

signature dependence in the Coriolis interaction and not the residual $\pi - \nu$ interaction is responsible for the staggering[13]. Thus in the context of the particle plus rotor models, it is suggested that the mechanism behind the staggering entails an interaction of the particles with the core rather than among the valence particles themselves.

In the following we discuss the present experimental and theoretical situation within the framework of the proton-particle neutron-quasiparticle quadrupole vibrator model. In the next section we determine the parameters entering the calculation. Contrary to the case of the TQPRM, we are able to distinguish more clearly between the effects of the quadrupole phonon coupling and the residual valence proton-neutron interaction. A final test on the wave functions is provided by the calculation of the experimentally available magnetic dipole and electrical quadrupole moments.

3.2. *Parameters*

The model Hamiltonian is described in detail in Sect. 2. An appropriate basis for describing the negative parity intruder band can be contructed by the coupling

of proton — 1-particle — 2-hole neutron — one-quasiparticle excitations to the even-even Pb-core nuclei. Thereby we simplify the proton — 2-hole Pb-core coupled system by the corresponding even-even Hg vibrator spectrum. Thus, the basis wave functions are built from the coupling of the $1h_{9/2}(\pi)$-particle $1\tilde{i}_{13/2}(\nu)$-quasiparticle multiplet to the Hg vibrational core.

The quasiparticle energy and occupation probability of the $1\tilde{i}_{13/2}(\nu)$ quasi-neutron is obtained by a Bardeen-Cooper-Schrieffer (BCS) calculation, using the Nilsson Hamiltonian (in the spherical limit) and a constant pairing force[2]. The values of $\mu = 0.380$ and $\varkappa = 0.040$ were used[3]. The pairing strength $G(\nu)$ was adjusted in order to obtain the experimental odd-even mass differences. The result of this calculation are summarized in Tables 3 and 4. The neutron one-quasi-

TABLE 3.

N	$G(\nu)$	$\Delta(\nu)$
105	17.5	1.115
107	18.2	1.170
109	18.1	1.145
111	18.6	1.145
113	18.6	1.075
115	18.3	0.965
117	18.5	0.930
119	18.3	0.810
121	18.7	0.734
123	19.5	0.678
125	18.5	0.315

The pairing strength G (MeV) and the pairing gap Δ (MeV) (as determined from the experimental odd-even mass differences). The pairing strength G was adjusted to reproduce the pairing gap Δ. ($\mu = 0.380$, $\varkappa = 0.064$).

TABLE 4.

	v^2				$u^2 - v^2$			
N	$1i13/2(\nu)$	$2f5/2(\nu)$	$2p3/2(\nu)$	$2p1/2(\nu)$	$1i13/2(\nu)$	$2f5/2(\nu)$	$2p3/2(\nu)$	$2p1/2(\nu)$
105	0.46	0.09	0.17	0.05	0.08	0.82	0.67	0.91
107	0.54	0.12	0.22	0.06	−0.09	0.76	0.57	0.89
109	0.62	0.14	0.26	0.06	−0.25	0.72	0.48	0.87
111	0.70	0.17	0.33	0.08	−0.40	0.65	0.34	0.85
113	0.77	0.21	0.41	0.08	−0.55	0.58	0.18	0.83
115	0.85	0.25	0.51	0.09	−0.69	0.50	−0.01	0.83
117	0.89	0.34	0.63	0.11	−0.78	0.32	−0.27	0.78
119	0.93	0.45	0.76	0.12	−0.87	0.09	−0.53	0.76
121	0.96	0.63	0.86	0.17	−0.92	−0.26	−0.72	0.66
123	0.97	0.82	0.93	0.30	−0.95	−0.63	−0.86	0.40
125	1.00	0.97	0.99	0.60	−0.99	−0.95	−0.98	−0.20

The occupation probabilities $v^2(\nu)$ and the differences $[u^2(\nu) - v^2(\nu)]$ (as a function of neutron number N), calculated from the Nilsson model, including pairing.

particle energies are given in Fig. 4. The one-quasiparticle energies reproduce well the experimental trends of the corresponding ground and first excited states in the odd-mass Pb isotopes (Fig. 5).

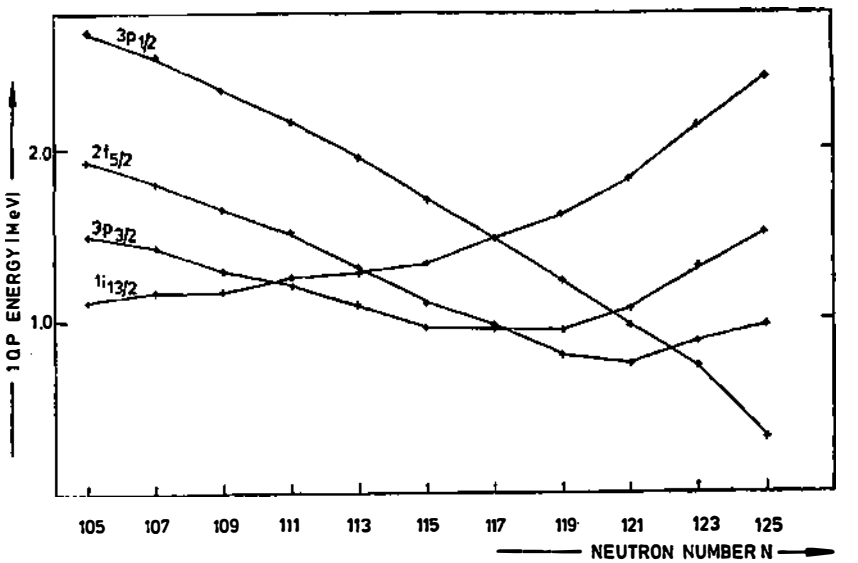

Fig. 4. Neutron one-qausiparticle energies for the Pb isotopes as a function of neutron-number.

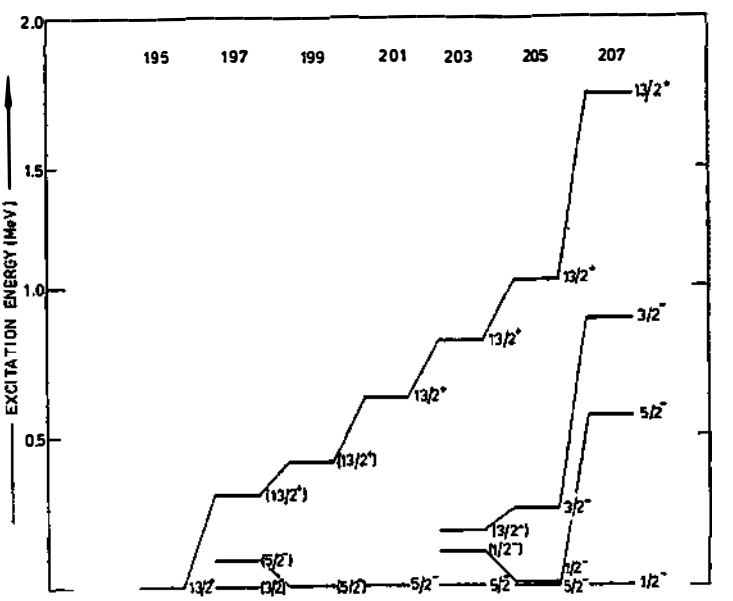

Fig. 5. Experimental energy levels with $J^{\pi} = 13/2^+, 5/2^-, 3/2^-, 1/2^-$ corresponding to the $1\tilde{i}_{13/2}$, $2\tilde{f}_{5/2}$, $3\tilde{p}_{3/2}$, $3\tilde{p}_{1/2}$ one-quasiparticle neutron states in the odd-even Pb isotopes[14].

The proton-neutron residual interaction was taken as a delta-function interaction i. e.

$$H_{int}(\pi, \nu) = -V_0 [(1 - \alpha) + \alpha \vec{\sigma_p} \cdot \vec{\sigma_n}] \delta(\vec{r_\pi} - \vec{r_\nu}), \tag{3.1}$$

with

$$V_0 = 300 \text{ MeVfm}^3 \quad \text{and} \quad \alpha = 0.25.$$

In Figs. 6.a, b, we represent the matrix elements of the interaction (3.1) for the $1h_{9/2}(\pi) - 1\tilde{i}_{13/2}(\nu)$ multiplet, taking $\alpha = 0.0$ and $\alpha = 0.5$. Since the $1\tilde{i}_{13/2}(\nu)$ neutron has a dominating hole character in the mass region considered, Fig. 6.a is the closest to the situation we are dealing with.

The value for the $\hbar\omega_2$-phonon energy in the even-even Hg nuclei, can be obtained directly from Fig. 3. The particle-core coupling strengths $\xi_2(\pi)$, $\xi_2(\nu)$ can in principle be obtained from a fit to the energy spectra of the neighbouring odd-even Tl and odd-even Hg isotopes respectively. In first approximation, we take $\xi_2(\pi) = \xi_2(\nu) = \xi_2$. Here ξ_2 is obtained starting from the experimental known $B(E2)$ values[15] of the underlying even-even Hg -cores, using a harmonic approximation

$$\xi_2 = \frac{4}{3} \frac{\sqrt{5\pi}}{\hbar\omega_2 Z R_0^2} \langle k \rangle B(E2; 2^+ \to 0^+)^{1/2}, \tag{3.2}$$

with R_0 the nuclear radius and $\langle k \rangle \cong 50$ MeV[16].
Hence, we obtain values for ξ_2 ranging from about 3 to 7 in going from ^{204}Hg to ^{196}Hg.

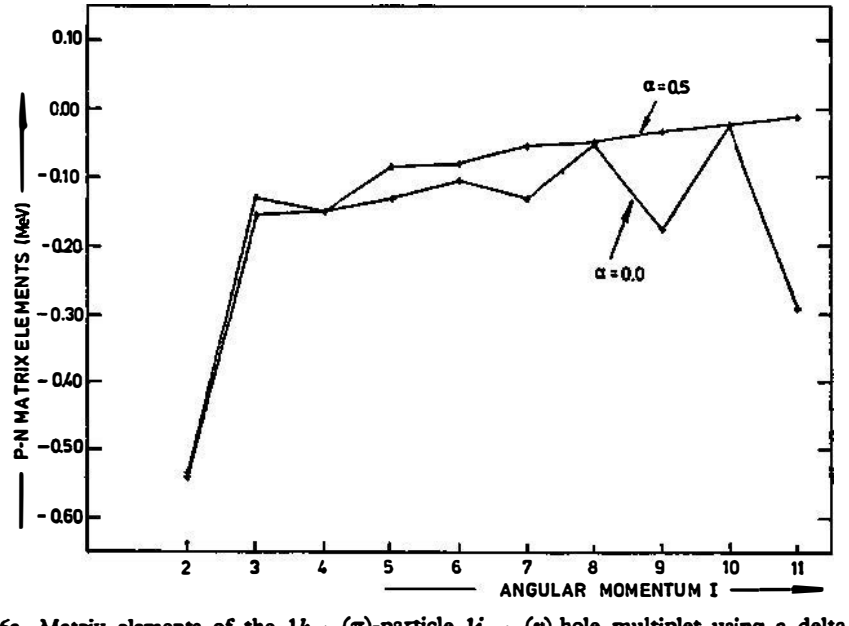

Fig. 6a. Matrix elements of the $1h_{9/2}(\pi)$-particle $1i_{13/2}(\nu)$-hole multiplet using a delta-force with spin-exchange ($V_0 = 300$ MeVfm^3, $\alpha = 0$ and $\alpha = 0.5$).

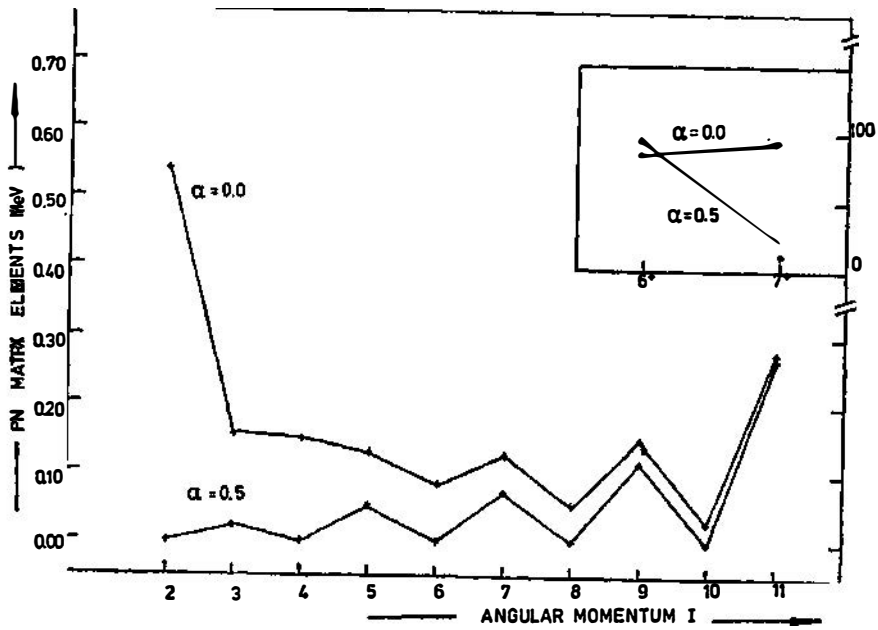

Fig. 6b. Same caption as Fig. 6a but for the $1h_{9/2}$ (π)-particle $1\tilde{i}_{13/2}$-particle multiplet.

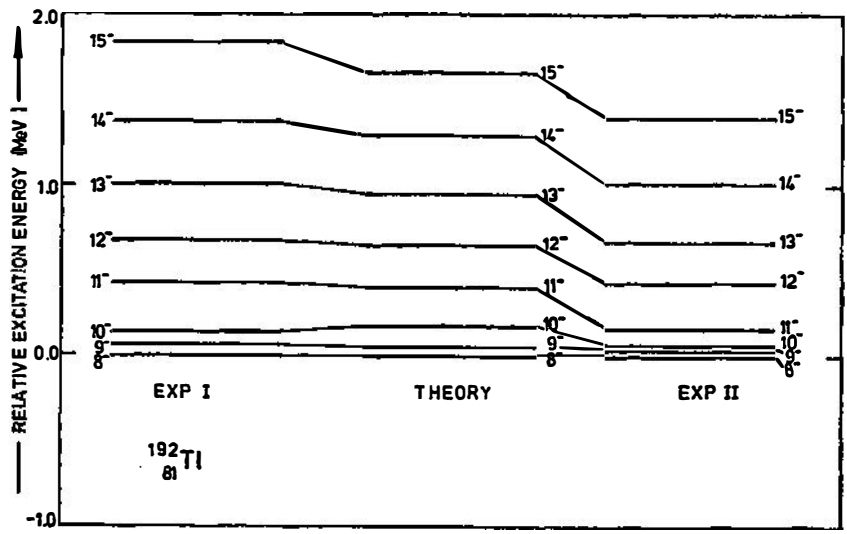

Fig. 7. The $1h_{9/2}^{-1}$ (π) — $1\tilde{i}_{13/2}$ (ν) negative parity band in ^{192}Tl, theory versus experiment. Up to four quadrupole phonon states are taken into account ($\hbar\omega_2 = 0.5$ MeV, $\xi_2(\pi) = \xi_2(\nu) = 7$). A delta-force with spin-exchange ($V_0 = 300$ MeVfm^3, $a = 0$ and $a = 0.5$). Experiment (II) corresponds to the case where no (an) unobserved low-energy transition is included (see Tables 1 and 2).

3.3. *Results and discussion*

As an example, a detailed calculation of the level scheme for ^{192}Tl is performed (Fig. 7). The value of $\hbar\omega_2$ was taken as:

$$\hbar\omega_2 = \frac{E_x(4_1^+)\ ^{192}\mathrm{Tl})}{2} > E_x(2_1^+)\,(^{192}\mathrm{Hg}). \tag{3.3}$$

Here $E_x(4_1^+)$, $E_x(2_1^+)$ denotes the two- and one phonon energy, respectively. This choice for $\hbar\omega_2$ which is slightly different from $E_x(2_1^+)$, results in a more expanded band, especially the upper part of band. It also takes into account the fact that the experimental two-phonon states in the underlying even-even Hg-core are somewhat higher than two times the experimental one-phonon level (as expressed by the inequality in equation (3.3)). The coupling strength ξ_2 was taken equal to 7. Fig. 6.a explains the bunching of the lower bandlevels ($J^\pi \leq 10$) due to the used delta proton-neutron force with spin-exchange. This conclusion is not changed by the fact all these lowest multiplet members contain almost the same one-phonon admixture (Table 5). Both the quadrupole-core coupling and the proton-

TABLE 5.

$$|8^-\rangle \cong 0.38\,|(1,2)\times 9_1^-(\pi\nu)\rangle + 0.37\,|(0,0)\times 8_1^-(\pi\nu)\rangle - 0.35\,|(1,2)\times 7_1^-(\pi\nu)\rangle + 0.30\,|(2,0)\times 8_1^-(\pi\nu)\rangle$$

$$|9^-\rangle \cong -0.42\,|(1,2)\times 8_1^-(\pi\nu)\rangle + 0.36\,|(0,0)\times 9_1^-(\pi\nu)\rangle + 0.32\,|(1,2)\times 10_1^-(\pi\nu)\rangle$$

$$|10^-\rangle \cong -0.46\,|(1,2)\times 9_1^-(\pi\nu)\rangle + 0.32\,|(0,0)\times 10_1^-(\pi\nu)\rangle$$

$$|11^-\rangle \cong -0.41\,|(1,2)\times 10_1^-(\pi\nu)\rangle - 0.31\,|(2,2)\times 9_1^-(\pi\nu)\rangle + 0.32\,|(2,4)\times 8_1^-(\pi\nu)\rangle$$

$$|12^-\rangle \cong 0.49\,|(2,4)\times 9_1^-(\pi\nu)\rangle - 0.38\,|(1,2)\times 10_1^-(\pi\nu)\rangle$$

$$|13^-\rangle \cong 0.52\,|(2,4)\times 10_1^-(\pi\nu)\rangle - 0.37\,|(3,6)\times 9_1^-(\pi\nu)\rangle - 0.32\,|(4,8)\times 5_1^-(\pi\nu)\rangle - 0.30\,|(1,2)\times 11_1^-(\pi\nu)\rangle$$

$$|14^-\rangle \cong 0.53\,|(4,8)\times 6_1^-(\pi\nu)\rangle - 0.51\,|(2,4)\times 10_1^-(\pi\nu)\rangle$$

$$|15^-\rangle \cong 0.64\,|(3,6)\times 10_1^-(\pi\nu)\rangle - 0.50\,|(2,4)\times 11_1^-(\pi\nu)\rangle - 0.32\,|(4,8)\times 9_1^-(\pi\nu)\rangle$$

Wave functions for ^{192}Tl (|amplitudes| ≥ 0.30). The used basis is $|(N,R)\times I_i^\pi(\pi\nu)\rangle$, N the number of quadrupole phonons, R is the collective angular momentum, $I_i^\pi(\pi\nu)$ is the state obtained from coupling the $1h_{9/2}(\pi)$ particle to the $1\tilde{i}_{13/2}(\nu)$ quasiparticle.

neutron interaction produce a smooth reduction of the multiplet splitting of the lower band member, which is proportional to the $(u^2 - v^2)\,(1\tilde{i}_{13/2}(\nu))$ behaviour. Since $(u^2 - v^2)\,(1\tilde{i}_{13/2}(\nu))$ decreases with decreasing neutron-number (see Table 4), the corresponding multiplet states get compressed and a level crossing occurs when $(u^2 - v^2)\,(1\tilde{i}_{13/2}(\nu))$ becomes negative. Fig. 8 provides a global but schematic explanation for the observed level crossing. For all values of $v^2\,(1\tilde{i}_{13/2}(\nu))$, a constant value of $\hbar\omega_2 = 0.4$ MeV and $\xi_2 = 2.5$ was used. This choice for the collective parameters gives the best prediction for the experimental level crossing

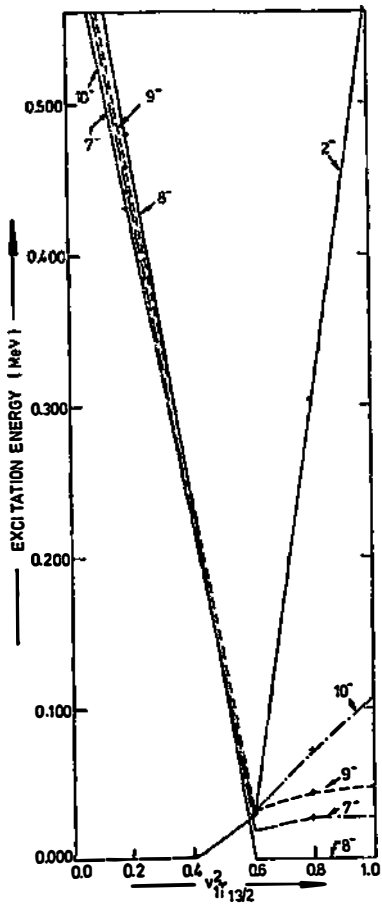

Fig. 8. Relative energy position of the 7^-, 8^-, 9^-, 10^-, (2^-) states of the $1h^{-1}_{9/2}(\pi) - \widetilde{1i}_{13/2}(\nu)$ multiplet as a function of $v^2(1i_{13/2}(\nu))$. The multiptet is coupled to the quadrupole vibrations of the underlying even-even Hg core ($\hbar\omega_2 = 0.4$ MeV, $\xi_2(\pi) = \xi_2(\nu) = 2.5$, up to 4 quadrupole phonons are taken into account). The proton-neutron interaction used, is a delta-force with spin-exchange ($V_0 = 300$ MeVfm^3, $\alpha = 0.25$).

i. e. at $v^2(\widetilde{1i}_{13/2}(\nu)) \cong 0.4$—$0.5$. In other words, a level crossing occurs in the $^{186-188}$Tl isotopes, corresponding to $v^2(\widetilde{1i}_{13/2}(\nu)) \cong 0.4$—$05$. The fact that the 8^- state lies below the 10^- state for $v^2(\widetilde{1i}_{13/2}(\nu)) > 0.5$, can be ascribed to the admixtures of the quadrupole phonons in the first few levels of the band. According to the parabolic rule[5], the state with

$$J = [j_\pi(j_\pi + 1) + j_\nu(j_\nu + 1) - 1/4]^{1/2} - 1/2 \simeq 8 \tag{3.4}$$

should be the lowest. When calculating the position of the energy levels in Fig. 8, but now without quadrupole phonons, the π-ν interaction (see Fig. 6.a) favours

the 10^- to be the lowest multiplet state. The result is presented in Fig. 9. In first approximation, this corresponds to the situation in the odd-odd Bi isotopes[17-21], where the 10^- state should be the lowest multiplet state (Fig. 10). The decrease of the excitation energy of the 10^- isomer in the Bi-isotopes with decreasing neutron-number is related to the one-quasiparticle energy of the $1\tilde{i}_{13/2}(\nu)$ orbit relative to the lowest neutron quasiparticle state (the proton particle remaining in the $1h_{9/2}(\pi)$ state for both the ground state and the 10^- isomer). The decreasing behaviour of the $E(\tilde{i}_{13/2}(\nu))$ quasiparticle energy with decreasing neutron-number is confirmed by Figs. 4 and 5.

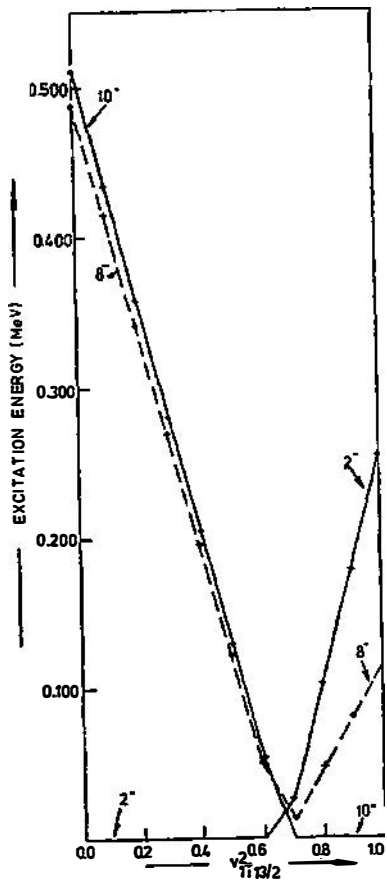

Fig. 9. Relative energy position of the 10^- and 8^- states of the $1h_{9/2}^{-1}(\pi) - 1\tilde{i}_{13/2}(\nu)$ multiplet as a function of $v^2(1\tilde{i}_{13/2}(\nu))$. A proton-neutron delta-force with spin-exchanges is used (same parameters as Fig. 8), however no quadrupole phonon excitations are included in the calculation.

Returning to the negative parity band in the Tl-isotopes, it is noted from Fig. 6.a that the 11^- state lies well separated from the lower-lying close-lying multiplet members. Hence the 11^- state should be situated much higher in energy

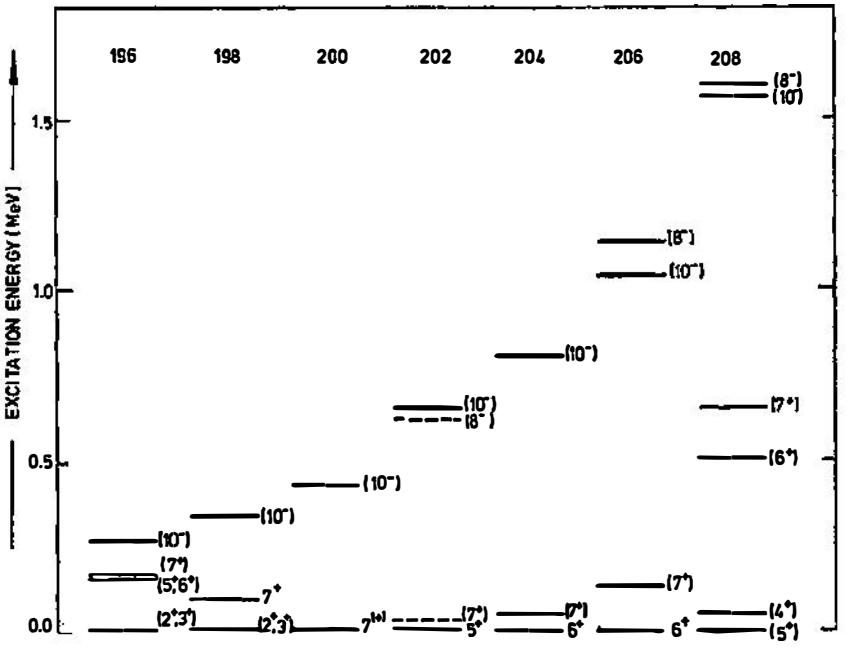

Fig. 10. Energy level systematics of the 10^- isomeric states in odd-odd Bi isotopes.

than the other multiplet states. Since the 11^- (10^-) wave function contains important one- and two-phonon (zero- and one-phonon) admixtures (Table 5), the $(E(11^-) - E(10^-))$ energy difference as a function of neutron-number is closely related to the corresponding $E(2_1^+)$-phonon energy (Fig. 3). We remark that the

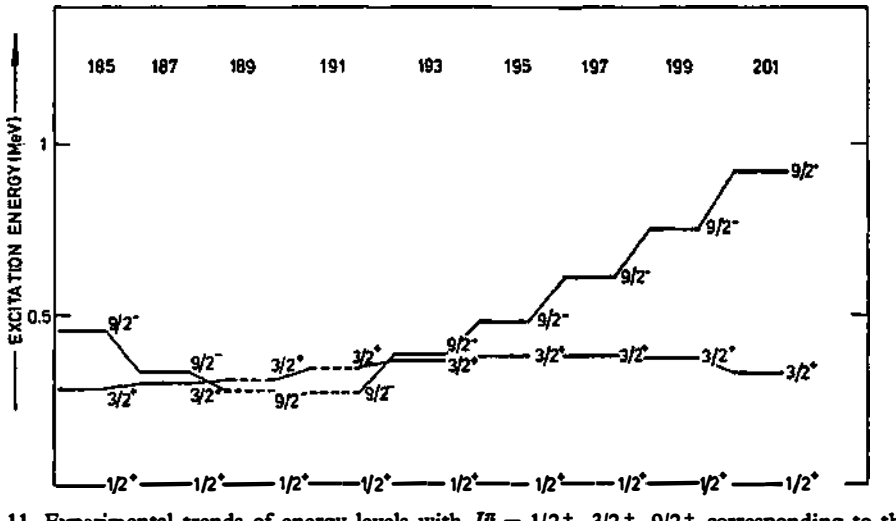

Fig. 11. Experimental trends of energy levels with $J^\pi = 1/2^+$, $3/2^+$, $9/2^+$ corresponding to the $3s_{1/2}$, $2d_{3/2}$ and $1h_{9/2}$ proton-particle states in the odd-even Tl isotopes[14].

energy difference between the bandhead and the 7^+ level (mainly $3s^{-1}_{1/2}(\pi) - 1\tilde{i}_{13/2}(\nu)$ configuration) follows the trend of the $(E(9/2^-) - E(1/2^+))$ energy difference in the neighbouring odd-even Tl isotopes (see Fig. 11)[22].

Finally, in Fig. 2 we observe that the theoretical transition energies in ^{192}Tl exhibit no staggering within the framework of the particle-vibrator model. Due to the different interactions (π-ν, π-core, ν-core) no simple conclusions can be drawn about staggering. Moreover, in the lighter $^{186-190}$Tl isotopes and in ^{200}Tl, the experimental transition energies show no staggering at all.

3.4. *Electromagnetic properties*

In Table 6, we compare experimental magnetic g-factors with the calculated values in both the odd-odd Bi and odd-odd Tl isotopes. We recall that the leading contribution to the magnetic g-factor contain no explicit dependence on the BCS-occupation probability $v^2(1\tilde{i}_{13/2}(\nu))$. So, for the Bi-isotopes we calculated the magnetic g-factor using the same $v^2(1\tilde{i}_{13/2}(\nu)) = 1.0$. A detailed study should require more experimental information. In the case of ^{192}Tl almost no effect was observed on the calculated g-factors, using wave functions for the 8^- state

TABLE 6.

	$J\pi$	Experiment	Theory
^{202}Bi	10^-	0.255(3)[19]	
^{204}Bi	10^-	0.236(23)[19]	
^{206}Bi	10^-	0.2642(14)[17]	0.233
^{208}Bi	10^-	0.2666(27)[18]	
^{192}Tl	8^-	0.207(5)[23]	0.171

Comparison of the experimental g-factors with the theoretical prediction. As effective single-particle g-factors we take: $g_l(\pi) = 1.00\mu_N$, $g_l(\nu) = 0.00\mu_N$, $g_s(\pi) = +2.7928\mu_N$, $g_s(\nu) = -1.91315\mu_N$. For the Bi isotopes $v^2(1i_{13/2}(\nu))$ was taken equal to 1.00. For ^{192}Tl, the value $v^2(1i_{13/2}(\nu)) = 0.70$ was used.

TABLE 7.

ξ_2	$Q(8^-)$ (efm^2)
7	73
5	63
3.5	50
2.5	38

Quadrupole moment of 8^- bandhead for different values of the coupling strength ξ_2. A constant value for $e_{vib} = 4e$ is used. The occupation probability is taken $v^2 = 0.7$, corresponding to ^{192}Tl ($e\pi = 1.5e$, $e\nu = 0.5e$).

obtained with different values for the coupling strength ξ_2. The g-factor is rather insensitive to the collectivity of the wave function, but rather reflects the degree of configuration mixing of the valence particles.

On the contrary, the quadrupole moment depends largely on the degree of collectivity of the wave functions. This is illustraed in Table 7. The quadrupole moments are calculated using wave functions corresponding to different values of ξ_2. The same value of $e_{vib} = 4e$ is used. Changing e_{vib}, according to the relation

$$e_{vib} = \xi_2 \sqrt{\frac{\pi}{5}} \frac{Ze\hbar\omega_2}{\langle k \rangle}, \tag{3.5}$$

with $\langle k \rangle \cong 50$ MeV[16], would even enlarge this effect. A preliminary experimental value of 45(9) e^2fm^2 for the quadrupole moment for the 8^- state in ^{192}Tl was obtained[23].

In Table 8, we give the intra-band $B(M1)$ and $B(E2)$ values. The comparison with experimental values would confirm whether the selected theoretical levels correspond to the experimental ones. It would permit us to give a more precise definition of the observed collective band in terms of levels connected through transitions with a certain behaviour of the $B(M1)$, $B(E2)$ values.

TABLE 8.

I^π	$B(M1; I \to I-1) \cdot (\mu_N^2)$	$B(E2; I \to I-1) \cdot (e^2 fm^4)$
9^-	1.73	8400
10^-	1.43	8400
11^-	1.07	7510
12^-	0.678	4510
13^-	0.832	4730
14^-	0.482	2660
15^-	0.655	2820

Theoretical $B(M1)$ and $B(E2)$ values for intra-band transition in the case of ^{192}Tl ($g_l(\pi) = 1\mu_N$, $g_l(\nu) = 0\mu_N$, $g_s(\pi) = 2.7928\mu_N$, $g_s(\nu) = -1.91315\mu_N$, $g_R = Z/A$, $e_\pi = 1.5e$, $e_\nu = 0.5e$, $e_{vib} = 4e$).

4. *Conclusion*

Using an approach based on a quadrupole vibrator coupled to proton-neutron quasiparticle multiplets, we were able to give a description of the observed properties of the $1h_{9/2}^{-1}(\pi) - 1\tilde{i}_{13/2}(\nu)$ intruder negative parity band in the odd-odd Tl nuclei. The energy spectrum of the negative parity band in the Tl isotopes, could be related to the energy levels in the neighbouring Pb, Tl and Bi isotopes. A more detailed investigation of the intruder systematics in that region[24], shows that the intruder negative parity band in odd-od $^{186-200}$Tl isotopes completes the picture on intruder-based bands in that region.

Acknowledgements

The authors are grateful to V. Paar for inviting us to write an article for this memorial volume. They both owe a lot to the late G. Alaga for much inspiration along the way to study nuclear structure, keeping away from too formal developments but accentuating the importance for elegant mathematics, intuitive methods and staying in contact with the world of experimental data, three aspects of research which were present in a well balanced way in the person of G. Alaga.

APPENDIX

Derivation of the parabolic rule

We derive an analytical expression of the energy splitting of a proton-neutron multiplet $|(pn)I|\rangle$, $I = |j_p - j_n|, \ldots, j_p + j_n$, coming from the exchange of quadrupole phonons.

The second order perturbation theory gives following expression:

$$\Delta E(I) = -\frac{1}{\hbar\omega_2} \sum_{p'n'I'} |\langle (1,2) \times (p'n')\, I'; IM| H_{coupl} |(0,0) \times (pn)\, I; IM\rangle|^2, \tag{A.1}$$

with

$$H_{coupl} = H_{coupl}(\pi) + H_{coupl}(\nu) = -\sqrt{\frac{\pi}{5}}\, \hbar\omega_2 (\xi_2(\pi)\, Y_2(\pi) + \xi_2(\nu)\, Y_2(\nu)) \cdot Q_2(coll),$$
$$Q_{2\mu}(coll) = b^+_{2\mu} + (-1)^\mu b_{2-\mu}, \tag{A.2}$$

$b_{2\mu}$ = quadrupole phonon creation operator.

Here $|(N,R) \times (pn)\, I; IM\rangle$ is the wave function describing the coupling of the collective vibrations to the proton-neutron excitations, where N represents the number of quadrupole phonons, R is the collective angular momentum, and $|(pn)\, I\rangle$ denotes the proton-neutron multiplet coupled to total angular momentum I. More explicitely we have:

$$|(pn)\, IM\rangle = \sum_{m_p m_n} \langle j_p m_p j_n m_n | IM\rangle\, c^+_{nm_n}(\nu)\, c^+_{pm_p}(\pi) \widetilde{|}0\rangle, \tag{A.3}$$

with

$c^+_{xm_x}(\varrho)$ = quasiparticle creation operator, $(x = p, n;\ \varrho = \pi, \nu)$,

$\widetilde{|0\rangle}$ = Bardeen-Cooper-Schrieffer (BSC) vacuum,

$p \equiv n_p l_p j_p, \qquad n \equiv n_n l_n j_n.$

The matrix element in equation (A.1) becomes:

$$\langle (1,2) \times (p'n')\, I'; IM | \, H_{coupl}(\pi) + H_{coupl}(\nu) \, | (0,0) \times (pn)\, I; IM \rangle =$$

$$= - \sqrt{\frac{\pi}{5}}\, \hbar\omega_2 \left\{ (-1)^{I'+J} \begin{Bmatrix} 2 & I' & J \\ I & 0 & 2 \end{Bmatrix} \langle (1,2) | \, | Q_2(coll) | \, | (0,0) \rangle \right.$$

$$\left. \times \langle (p'n')\, I' | \, | \xi_2(\pi)\, Y_2(\pi) + \xi_2(\nu)\, Y_2(\nu) | \, | (pn)\, I \rangle \right\}. \qquad \text{(A.4)}$$

For the single-particle reduced matrix elements, we obtain:

$$\langle (p'n')\, I' | \, | \xi_2(\pi)\, Y_2(\pi) + \xi_2(\nu)\, Y_2(\nu) | \, | (pn)\, I \rangle =$$

$$= (-1)^{j'_p + j'_n + I} \sqrt{(2I'+1)(2I+1)}\, \langle j''_p | \, | Y_2(\pi) | \, | j_p \rangle \begin{Bmatrix} j''_p & I' & j'_n \\ I & j_p & 2 \end{Bmatrix} \delta_{n',n} +$$

$$+ (-1)^{j'_p + j_n + I'} \sqrt{(2I'+1)(2I+1)}\, \langle j''_n | \, | Y_2(\nu) | \, | j_n \rangle \begin{Bmatrix} j''_n & I' & j''_p \\ I & j_n & 2 \end{Bmatrix} \delta_{p',p}. \qquad \text{(A.5)}$$

We also have:

$$\begin{Bmatrix} 2 & I' & I \\ I & 0 & 2 \end{Bmatrix} = \frac{(-1)^{I'+I}}{\sqrt{5}\sqrt{2I+1}} \qquad \text{(A.6)}$$

and

$$\langle (1,2) | \, | Q_2(coll) | \, | (0,0) \rangle = \sqrt{5}. \qquad \text{(A.7)}$$

Combining the above expressions, we can write:

$$\Delta E(I) = - \frac{1}{\hbar\omega_2} \sum_{p'n'I'} \left| - \sqrt{\frac{\pi}{5}}\, \hbar\omega_2 \left(\xi_2(\pi) (-1)^{j'_p + j'_n + I} \sqrt{2I'+1} \right.\right.$$

$$\times \begin{Bmatrix} j'_p & I' & j''_n \\ I & j_p & 2 \end{Bmatrix} \langle j''_p | \, | Y_2(\pi) | \, | j_p \rangle \delta_{n',n} + \xi_2(\nu) (-1)^{j''_p + j'_n + I'} \sqrt{2I'+1}$$

$$\left.\left. \times \begin{Bmatrix} j''_n & I' & j''_p \\ I & j_n & 2 \end{Bmatrix} \langle j''_n | \, | Y_2(\xi) | \, | j_n \rangle \delta_{p',p} \right) \right|^2. \qquad \text{(A.8)}$$

The last equation can be separated as follows:

$$\Delta E(I) = \Delta E_a + \Delta E_b(I), \qquad \text{(A.9)}$$

with

$$\Delta E_a = - \frac{\pi}{5} \hbar\omega_2 \left\{ \sum_{p'I'} \xi_2^2(\pi) (2I'+1) \begin{Bmatrix} j'_p & I & j_n \\ I & j_p & 2 \end{Bmatrix}^2 \langle j''_p | \, | Y_2(\pi) | \, | j_p \rangle^2 + \right.$$

$$+ \sum_{n'I'} \xi_2^2(\nu)(2I'+1)\begin{Bmatrix} j' & I & j_p \\ I & j_n & 2 \end{Bmatrix}^2 \langle j_n' || Y_2(\nu) || j_n \rangle^2 \Big\} =$$

$$= -\frac{\pi}{5}\hbar\omega_2 \left\{ \frac{1}{2j_p+1} \sum_{p'} \xi_2^2(\pi) \langle j_p'' || Y_2(\pi) || j_p \rangle^2 + \right.$$

$$\left. \frac{1}{2j_n+1} \sum_{n'} \xi_2^2(\nu) \langle j_n' || Y_2(\nu) || j_n \rangle^2 \right\}. \tag{A.10}$$

In (A.10), we used the orthogonality relation of the 6-j symbols[25,26]. We clearly see that ΔE_a is independent of I, and is only causing an overall shift of the multiplet. Only contribution ΔE_b gives rise to the splitting of the multiplet:

$$\Delta E_b(I) = -\frac{2\pi}{5}\hbar\omega_2\, \xi_2(\pi)\, \xi_2(\nu) \sum_{I'} (2I'+1)(-1)^{I+I'} \begin{Bmatrix} j_p & I' & j_n \\ I & j_p & 2 \end{Bmatrix}$$

$$\times \begin{Bmatrix} j_n & I' & j_p \\ I & j_n & 2 \end{Bmatrix} \langle j_p || Y_2(\pi) || j_p \rangle \langle j_n || Y_2(\nu) || j_n \rangle$$

$$= -\frac{2\pi}{5}\hbar\omega_2\, \xi_2(\pi)\, \xi_2(\nu)\, (-1)^{j_p+j_n+I} \begin{Bmatrix} j_p & j_p & 2 \\ j_n & j_n & I \end{Bmatrix}$$

$$\times \langle j_p || Y_2(\pi) || j_p \rangle_{(qp)} \langle j_n || Y_2(\nu) || j_n \rangle_{(qp)}. \tag{A.11}$$

We used the sum rule for 6-j symbols:

$$\sum (-1)^{j+j'+j''}(2j+1) \begin{Bmatrix} j_1 & j_2 & j' \\ j_3 & j_4 & j \end{Bmatrix} \begin{Bmatrix} j_1 & j_3 & j'' \\ j_2 & j_4 & j \end{Bmatrix} = \begin{Bmatrix} j_1 & j_2 & j' \\ j_4 & j_3 & j'' \end{Bmatrix}. \tag{A.12}$$

Taking into account following analytical expression for the 3-j symbols[27]:

$$\begin{Bmatrix} j_p & j_p & 2 \\ j_n & j_n & I \end{Bmatrix} = (-1)^{j_p+j_n+I} \cdot 6 \cdot \left[A(A+1) - \frac{4}{3} j_p(j_p+1) j_n(j_n+1) \right]$$

$$\times [(2j_p+3)(2j_p+2)(2j_p+1)(2j_p)(2j_p-1)(2j_n+3)$$

$$\times (2j+2)(2j_n+1)(2j_n)(2j_n-1)]^{-1/2}, \tag{A.13}$$

with $A = I(I+1) - j_p(j_p+1) - j_n(j_n+1)$, and the analytical expression for the reduced matrix elements of the spherical harmonic in the coupled representation $\vec{l} + \vec{s} = \vec{j}$:

$$\langle j || Y_2 || j \rangle_{(qp)} = (u_j^2 - v_j^2)(2j+1) \sqrt{\frac{5}{4\pi}} \frac{(3/4 - j(j+1))}{\sqrt{(2j-1)\, j\, (2j+1)\, (j+1)\, (2j+3)}}, \tag{A.14}$$

we finaly obtain:

$$\Delta E_b(I) = \xi_2(\pi)\,\xi_2(\nu)\,\hbar\omega_2\left(-\frac{3}{4}\left(\frac{[I(I+1)-j_p(j_p+1)-j_n(j_n+1)]^2}{(2j_p)(2j_n)(2j_p+2)(2j_n+2)}+\right.\right.$$

$$\left.\left.+\frac{[I(I+1)-j_p(j_p+1)-j_n(j_n+1)]}{(2j_p)(2j_n)(2j_p+2)(2j_n+2)}\right)+\frac{1}{16}\right)\Theta(p)\,\Theta(n), \qquad \text{(A.15)}$$

and $\Theta(x) = (u^2(x) - v^2(x))$, $x = p, n$.

The energy splitting of the proton-neutron multiplet due to the exchange of the quadrupole phonon is given by:

$$-\frac{3}{4}\,\xi_2(\pi)\,\xi_2(\nu)\,\hbar\omega_2\,\cdot$$

$$\frac{[I(I+1)-j_p(j_p+1)-j_n(j_n+1)]^2+[I(I+1)-j_p(j_p+1)-j_n(j_n+1)]}{(2j_p)(2j_n)(2j_p+2)(2j_n+2)}\,\Theta, \qquad \text{(A.16)}$$

with $\Theta = \Theta(p)\,\Theta(n)$.

Expression (A.16) represents a parabola as a function of $I(I+1)$.

References

1) G. Alaga in *Cargèse Lect. in Physics*, Vol. 3, ed. M. Jean (Gordon and Breach Sc. Publ., 1969), p 579; G. Alaga in *Proc. of the Int. School of Physics »Enrico Fermi«*, course XL, eds. M. Jean and R. A. Ricci (Academic Press, 1969), p 28;
2) P. Ring and P. Schuck, *The Nuclear Many-Body Problem* (Springer, Berlin, 1980);
3) J. Moreau, Lic. thesis, Rijksuniversiteit Gent, 1980;
4) J. Sau, K. Heyde, Phys. Rev. **C23** (1981) 2315;
5) V. Paar, Nucl. Phys. **A331** (1979) 16;
6) A. J. Kreiner, M. Fenzl, S. Lunardi and M. A. J. Mariscotti, Nucl. Phys. **A282** (1977) 243;
7) H. Toki, H. L. Yadav and A. Faessler, Phys. Lett. **71B** (1977) 1;
8) A. J. Kreiner, M. Fenzl and W. Kutschera, Nucl. Phys. **A308** (1978) 147;
9) A. J. Kreiner, M. Fenzl, U. Heim and W. Kutschera, Phys. Rev. **C20** (1979) 2205;
10) A. J. Kreiner, A. Filevich, G. Garcia Bermudez, M. A. J. Mariscotti, C. Baktash, E. der Mateosian and P. Thieberger, Phys. Rev. **C21** (1980) 933;
11) A. J. Kreiner, Phys. Rev. **C22** (1980) 2570;
12) A. J. Kreiner, M. A. J. Mariscotti, C. Baktash, E. der Mateosian and P. Thieberger, Phys. Rev. **C23** (1981) 748;
13) A. J. Kreiner, C. Baktash, G. Garcia Bermudez and M. A. J. Mariscotti, Phys. Rev. Lett. **47** (1981) 1709;
14) C. M. Lederer and V. S. Shirly, *Tables of Isotopes*, Wiley interscience, N. Y. (1978);
15) C. K. Ross and R. K. Bhaduri, Nucl. Phys. **A196** (1976) 369;
16) K. Heyde and P. J. Brussaard, Nucl. Phys. **A104** (1967) 81;
17) G. Schärfer, H. Hübel, C. Günther, A. Goldman and D. Riegel, Phys. Lett. **46B** (173) 65;
18) H. Hübel, C. Günther, K. Euler, N. Bräner and D. Riegel, Nucl. Phys. **A227** (1974) 421;
19) A. Kleinrahm, C. Günther, H. Hübel and B. V. Thirumala Rao, Nucl. Phys. **A346** (1980) 324 and references therein;

20) B. V. Thirumala Rao, R. Broda, C. Günther, A. Kleinrahm and M. Ogawa, Nucl. Phys. **A362** (1981) 71;
21) P. Van Duppen, private communication of preliminary results;
22) A. G. Smidth, R. L. Mlekodaj, E. L. Robinson, F. T. Avignone, J. Lin, G. M. Gowdy, J. L. Wood and R. W. Fink, Phys. Lett. **66B** (1977) 133;
23) A. Dafni, C. Broude, F. D. Davidovsky, M. Hass and G. Schatz, Nucl. Phys. **A383** (1981) 421;
24) M. Huyse, E. Coenen, K. Deneffe, P. Van Duppen, K. Heyde, J. Van Maldeghem, Phys. Lett. **201B** (1989) 293;
25) A. de-Shalit, I. Talmi, *Nuclear Shell Theory*, Academic Press (1963);
26) P. J. Brussaard, P. W. M. Glaudemans, *Shell Model Applications in Nuclear Spectroscopy*, North-Holland Publishing Company (1977);
27) L. C. Biedenharn, J. M. Blatt and M. E. Rose, Rev. of Modern Phys. **24** (1952) 212.

PROTONSKO-NEUTRONSKI MULTIPLETI U NEPARNO-NEPARNIM JEZGRAMA TALIJA

JORIS VAN MALDEGHEM i KRIS HEYDE

Institute of Nuclear Physics and Institute for Theoretical Physics, Proefituinstraat, Gent, Belgium

UDK 539.142

Originalni znanstveni rad

Koristeći vezanja čestice i sredice opisana je nuklearna struktura jezgara $^{186-200}$Tl. Istaknuta je važnost protonsko-neutronskih interakcija.